Available online at www.sciencedirect.com

ScienceDirect

Chinese Journal of Aeronautics 21(2008) 378-384

Chinese Journal of Aeronautics

www.elsevier.com/locate/cja

PID Controller Optimization by GA and Its Performances on the Electro-hydraulic Servo Control System

Karam M. Elbayomy*, Jiao Zongxia, Zhang Huaqing

School of Automation Science and Electrical Engineering, Beijing University of Aeronautics and Astronautics, Beijing 100083, China

Received 5 March 2008; accepted 6 June 2008

Abstract

A proportional integral derivative (PID) controller is designed and attached to electro-hydraulic servo actuator system (EHSAS) to control the angular position of the rotary actuator which control the movable surface of space vehicles. The PID gain parameters are optimized by the genetic algorithm (GA). The controller is verified on the new state-space model of servo-valves attached to the physical rotary actuator by SIMULINK program. The controller and the state-space model are verified experimentally. Simulation and experimental results verify the effectiveness of the PID controller adaptive by GA to control the angular position of the rotary actuator as compared with the classical PID controller and the compensator controller.

Keywords: PID controller; electro-hydraulic servo control system; genetic controller; GA

1 Introduction

Proportional integral derivative (PID) controllers are still the most popular ones in the processing industries. They are simple in structure, reliable in operation and robust in performances. One key factor for their success is that they act in the processes under control in a manner closely similar to human's natural responses to outside stimuli, that is the combined effects of spontaneity (proportional action), post training (integral action) and projection into future (derivative action).

The objectives of the PID controller are to control and improve the angular position response (the output) of the hydraulic rotary actuator. The PID controller implements the state-space model of the electro-hydraulic servo actuator system (EHSAS) to control the movable surface of space vehicle. The simulation, performed by SIMULINK program to check the effects of the PID controller on the EHSAS, uses the intelligent control, genetic algorithm (GA), to optimize the controller gain parameters K_p, K_i, and K_d on line. The experiment was carried out to verify the new state-space model which was used to design the controllers.

*Corresponding author. Tel.: +002-02-25554848.
E-mail address: karam_moh1@yahoo.com

2 System Description

The system consisted of a rotary actuator and a two-stage electro-hydraulic servo-valve with mechanical feedbacks as shown in Fig.1.

System Operation If an electrical control signal is applied to the coils (first stage), the resultant torque is proportional to the applied current. This torque causes the flapper plate to move and the throttle area of two regulating jets (nozzles) to change. For example, flapper's moving to the right increases the area of the left jet and decreases that of the right jet, and thus the pressure P_1 decreases while P_2 increases. The pressure difference ($\Delta P = P_2 - P_1$) increases in proportion to the flapper displacement. This pressure difference is the valve

output. The spool valve (second stage) is driven hydraulically by the pressure difference produced by the flapper valve. Thus the spool is displaced to the left connecting the port *A* of the rotary actuator to the high pressure and port *B* to the low pressure which rotate the wheel counterclockwise via the rightward displacement of the piston. The angular position is proportional to the input current. The maximum angular position for the rotary actuator is ±10°.

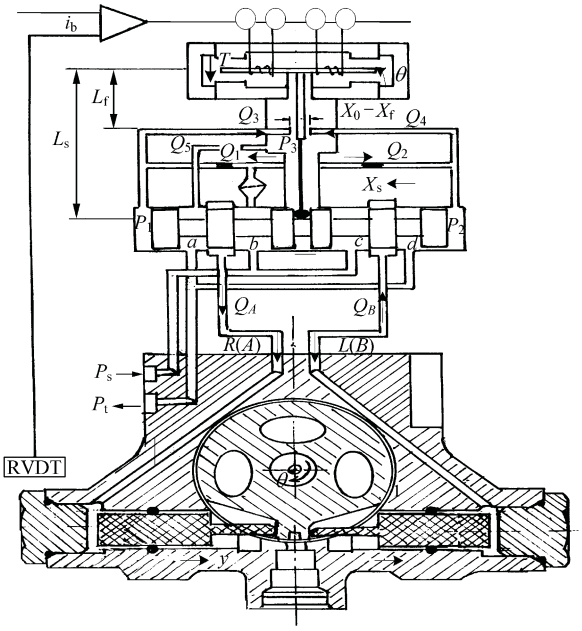

Fig.1 Cross-section of the rotary actuator and the two-stage servo-valve with mechanical feed-backs.

3 Mathematical Analysis and Model of Electro-hydraulic Servo-system

The design of stabilizing controllers used in nonlinear electro-hydraulic servo-systems has been extensively studied in recent years. Fig.1 shows a laboratory experimental electro-hydraulic servo-system driven by a hydraulic motor (rotary actuator) controlled by a servo-valve. In the system, the aerodynamic load acting on the fins' surfaces represents the outside load. The objective of the controller is to keep the angular position of the motor following a desired trajectory as precisely as possible. The entire system can be described by following equations.

3.1 Mathematical description of the motor torque

The torque of electromagnetic motors depends mainly on the coil currents and armature displacements. Neglecting the effects of magnetic hysteresis and the small term $K_\vartheta\vartheta$, the following expression that describes the motor torque mathematically is given by Ref.[1].

$$T = K_i i_e \tag{1}$$

The equation of motion of the armature includes the moment of inertia, damping coefficient, stiffness of flexural tubes, torque due to flapper displacements, limiter torque due to pressure forces and feedback torque.

$$T = J\frac{\mathrm{d}^2\vartheta}{\mathrm{d}^2t} + f_\vartheta\frac{\mathrm{d}\vartheta}{\mathrm{d}t} + K_T\vartheta + T_L + T_P + T_f \tag{2}$$

Suppose $|X_f| < X_{fL}$ then $T_L = 0$. The motor torque can be represented by

$$K_i i_e = J\frac{\mathrm{d}^2\vartheta}{\mathrm{d}^2t} + f_\vartheta\frac{\mathrm{d}\vartheta}{\mathrm{d}t} + K_T\vartheta + A_n P_L L_f + (\vartheta L_s + X)K_s L_s \tag{3}$$

3.2 Flow rate equations of flapper valve

In the steady state, the ports *A* and *B* are closed by the stationary spool, and then the steady state flow rates in the valve are Q_1, Q_2, Q_3, Q_4, and Q_5[2]. Assuming the supplied pressure is constant[2-3], the valve load pressure can be derived from the continuity equation:

$$\dot{P}_L = \frac{2\beta}{V_0}C_{12}\sqrt{\frac{P_s}{2}}\left[(1+\frac{X_f}{X_0})\sqrt{1-\frac{P_L}{P_s}} - \sqrt{1+\frac{P_L}{P_s}}\right] - \frac{2\beta A_s}{V_0}\frac{\mathrm{d}X}{\mathrm{d}t} \tag{4}$$

3.3 Mathematical description of the spool

The motion of the spool can be described by applying Newton's second law.

$$m_s\frac{\mathrm{d}^2X}{\mathrm{d}t} = A_s P - f_s\frac{\mathrm{d}X}{\mathrm{d}t} - (\vartheta L_s + X)K_s \tag{5}$$

Neglecting the transmission lines connecting the valve to the rotary actuator, the flow rates are Q_a, Q_b, Q_c, and Q_d[2]. Assuming the supplied pressure is

constant, the valve load pressure of the rotary actuator can be derived from the continuity equation:

$$\dot{P}_{\mathrm{PL}}=\frac{2\beta}{V_{\mathrm{C}}}\sqrt{\frac{P_{\mathrm{s}}}{\varsigma}}\left[C_{\mathrm{d}}A_{\mathrm{b}}(X)\sqrt{(1-\frac{P_{\mathrm{PL}}}{P_{\mathrm{s}}})}-C_{\mathrm{d}}A_{\mathrm{a}}(X)\sqrt{(1+\frac{P_{\mathrm{PL}}}{P_{\mathrm{s}}})}\right]-\frac{2\beta A_{\mathrm{P}}}{V_{\mathrm{C}}}\dot{Y} \tag{6}$$

3.4 Mathematical model of the hydraulic motor (special rotary actuator)

The dynamic equation of the piston is obtained by applying Newton's second law (see Fig.2).

$$P_{\mathrm{PL}}A_{\mathrm{P}}-F_{\mathrm{r}}-F_{\mathrm{C}}\,\mathrm{sgn}(Y)=m_{\mathrm{P}}\ddot{Y}+f_{\mathrm{P}}\dot{Y}+K_{\mathrm{P}}Y \tag{7}$$

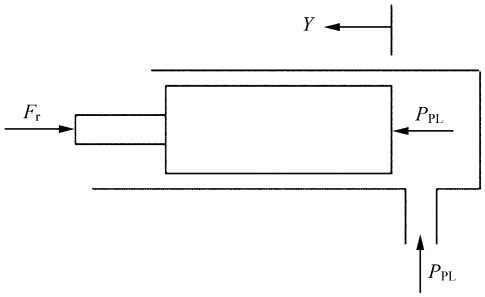

Fig.2 Applied force on the piston of the actuator.

Also, the dynamic equation of the rotor is obtained by applying Newton's second law to the rotating wheel as follows (see Fig.3). The Coulumb's friction exists between the piston and the rotary wheel; however, it is assumed to be acting on the piston because of the difficulty to measure it on each part individually.

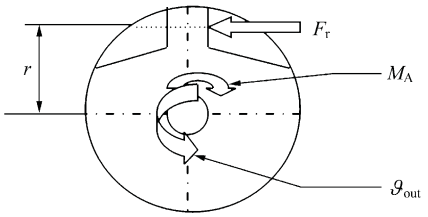

Fig.3 Applied force on the wheel of the actuator.

$$\sum M=F_{\mathrm{r}}r-M_{\mathrm{A}}$$

Then

$$F_{\mathrm{r}}r-M_{\mathrm{A}}=I\ddot{\vartheta}_{\mathrm{out}}+f\dot{\vartheta}_{\mathrm{out}}+K\vartheta_{\mathrm{out}} \tag{8}$$

where $M_{\mathrm{A}}=K_{\mathrm{M}}\vartheta_{\mathrm{out}}$, for small angle of rotation: $\vartheta_{\max}=\pm10^{\circ}=\pm0.174$ rad.

The relation between the piston displacement Y and the rotor output angle ϑ can be defined as

$$Y=r\vartheta_{\mathrm{out}} \tag{9}$$

Substituting Eqs.(8)-(9) into Eq.(7), the dynamic equation of the rotary actuator can be derived:

$$P_{\mathrm{PL}}A_{\mathrm{P}}=[m_{\mathrm{P}}r+\frac{I}{r}]\ddot{\vartheta}_{\mathrm{out}}+[f_{\mathrm{P}}r+\frac{f}{r}]\dot{\vartheta}_{\mathrm{out}}+[K_{\mathrm{P}}r+\frac{K+K_{\mathrm{M}}}{r}]\vartheta_{\mathrm{out}}+F_{\mathrm{C}}\,\mathrm{sgn}(\vartheta_{\mathrm{out}}) \tag{10}$$

4 State-space Representation of the Nonlinear Model of the Electro-hydraulic Servo-system

The nonlinear mathematical model of the system is described by Eqs.(3)-(6) and (10). The states of the system are described by the equations below:

$$\dot{X}_1=\dot{\vartheta}_{\mathrm{out}}=X_2 \tag{11}$$

$$\dot{X}_2=\ddot{\vartheta}_{\mathrm{out}}=\frac{1}{m_{\mathrm{P}}r+\frac{1}{r}}[A_{\mathrm{P}}X_3-(f_{\mathrm{P}}r+\frac{f}{r})X_2-(K_{\mathrm{P}}r+\frac{K}{r}+\frac{K_{\mathrm{C}}}{r})X_1-F_{\mathrm{C}}\,\mathrm{sgn}(X_1)] \tag{12}$$

$$\dot{X}_3=\dot{P}_{\mathrm{PL}}=\frac{2A_{\mathrm{r}}\beta C_{\mathrm{d}}}{V_{\mathrm{C}}}\sqrt{\frac{P_{\mathrm{s}}}{\zeta}}\left[(1+\frac{\pi D_{\mathrm{s}}}{A_{\mathrm{r}}}X_4)\cdot\sqrt{1-\frac{X_3}{P_{\mathrm{s}}}}-\sqrt{1+\frac{X_3}{P_{\mathrm{s}}}}\right]-\frac{2\beta A_{\mathrm{P}}}{V_{\mathrm{C}}}rX_2 \tag{13}$$

$$\dot{X}_4=\dot{X}_{\mathrm{s}}=X_5 \tag{14}$$

$$\dot{X}_5=\ddot{X}_{\mathrm{s}}=\frac{1}{m_{\mathrm{s}}}[A_{\mathrm{s}}X_6-f_{\mathrm{s}}X_5-K_{\mathrm{s}}(L_{\mathrm{s}}X_7+X_4)] \tag{15}$$

$$\dot{X}_6=\dot{P}_{\mathrm{L}}=\frac{2\beta C_{12}}{V_0}\sqrt{\frac{P_{\mathrm{s}}}{2}}\left[(1+\frac{L_{\mathrm{f}}X_7}{X_0})\cdot\sqrt{1-\frac{X_6}{P_{\mathrm{s}}}}-\sqrt{1+\frac{X_6}{P_{\mathrm{s}}}}\right]-\frac{2\beta A_{\mathrm{s}}}{V_0}X_5 \tag{16}$$

$$\dot{X}_7=\dot{\vartheta} \tag{17}$$

$$\dot{X}_8=\ddot{\vartheta}=\frac{1}{J}[iK_{\mathrm{i}}-f_{\vartheta}X_8-K_{\mathrm{T}}X_7-A_{\mathrm{n}}L_{\mathrm{f}}X_6-K_{\mathrm{s}}L_{\mathrm{s}}(L_{\mathrm{s}}X_7+X_4)] \tag{18}$$

5 Linear Mathematical Model of the System

The two load pressure Eqs.(4) and (6) for the valve and the rotary actuator respectively are linearized by binomial series into

$$\dot{P}_{\mathrm{L}}=\frac{2\beta}{V_0}C_{12}\sqrt{\frac{P_{\mathrm{s}}}{2}}(\frac{X_{\mathrm{f}}}{X_0}-\frac{P_{\mathrm{L}}}{P_{\mathrm{s}}})-\frac{2\beta A_{\mathrm{s}}}{V_0}\dot{X} \tag{19}$$

$$\dot{P}_{\mathrm{PL}}=\frac{2\beta}{V_{\mathrm{C}}}A_{\mathrm{r}}C_{\mathrm{d}}\sqrt{\frac{P_{\mathrm{s}}}{2}}\left(\frac{\pi D_{\mathrm{s}}X}{A_{\mathrm{r}}}-\frac{P_{\mathrm{PL}}}{P_{\mathrm{s}}}\right)-\frac{2\beta A_{\mathrm{P}}}{V_{\mathrm{C}}}\dot{Y} \quad (20)$$

The Eqs.(3), (5), (11), (19) and (20) represent the linear mathematical model of the system. The states of the linear system are chosen to be the same as those of non-linear system. Therefore, the state-space equations of the linear system will be:

$$\dot{X}_1=\dot{\vartheta}_{\mathrm{out}}=X_2 \quad (21)$$

$$\dot{X}_2=\ddot{\vartheta}_{\mathrm{out}}=\frac{1}{m_{\mathrm{P}}r+\frac{1}{r}}\left[A_{\mathrm{P}}X_3-\left(f_{\mathrm{P}}r+\frac{f}{r}\right)X_2-\left(K_{\mathrm{P}}r+\frac{K}{r}+\frac{K_{\mathrm{C}}}{r}\right)X_1\right] \quad (22)$$

$$\dot{X}_3=\dot{P}_{\mathrm{PL}}=\frac{2A_{\mathrm{r}}\beta C_{\mathrm{d}}}{V_{\mathrm{C}}}\sqrt{\frac{P_{\mathrm{s}}}{\zeta}}\left(\frac{\pi D_{\mathrm{s}}}{A_{\mathrm{r}}}X_4-\frac{X_3}{P_{\mathrm{s}}}\right)-\frac{2\beta A_{\mathrm{P}}}{V_{\mathrm{C}}}rX_2 \quad (23)$$

$$\dot{X}_4=\dot{X}_{\mathrm{s}}=X_5 \quad (24)$$

$$\dot{X}_5=\ddot{X}_{\mathrm{s}}=\frac{1}{m_{\mathrm{s}}}\left[A_{\mathrm{s}}X_6-f_{\mathrm{s}}X_5-K_{\mathrm{s}}(L_{\mathrm{s}}X_7+X_4)\right] \quad (25)$$

$$\dot{X}_6=\dot{P}_{\mathrm{L}}=\frac{2\beta C_{12}}{V_0}\sqrt{\frac{P_{\mathrm{s}}}{2}}\left(\frac{L_{\mathrm{f}}}{X_0}X_7-\frac{X_6}{P_{\mathrm{s}}}\right)-\frac{2\beta A_{\mathrm{s}}}{V_0}X_5 \quad (26)$$

$$\dot{X}_7=\dot{\vartheta} \quad (27)$$

$$\dot{X}_8=\ddot{\vartheta}=\frac{1}{J}\left[iK_{\mathrm{i}}-f_{\vartheta}X_8-K_{\mathrm{T}}X_7-A_{\mathrm{n}}L_{\mathrm{f}}X_6-K_{\mathrm{s}}L_{\mathrm{s}}(L_{\mathrm{s}}X_7+X_4)\right] \quad (28)$$

6 Controller Design

6.1 Introduction of PID controllers

PID controller is most commonly used in process control applications because of their relative ease of operation and satisfied performances[5]. Users can modify the dynamic properties of this controller by adjusting the three parameters: proportional, integral, and derivative.

Most of the previous study depend on rational transfer function or unreliable mathematical model, such as that of Chan and Hui[6], Zhang et al.[7]. They proposed an adaptive GA to tune the parameters of the PID controller and apply it in the sludge aeration process. Moradi[8] designed a predictive PID tuning to search for the optimal the parameters of the PID controller. Proposed by Yu and Hwang[9], the methodology of linear quadratic regulator was utilized to search for the optimal parameters of the PID controller. The whole design idea has been successfully realized on the speed control of a BLDC motor. Zou et al.[10] applied the particle swarm optimization (PSO) for PID parameters in hydraulic servo edger screw down system. Mookherjee[11] designed an analysis model for a single-stage electro-hydraulic servo-valve.

However in our controller, we use a new reliable analytical state-space model of the servo-valve attached to the physical rotary actuator (EHSAS) in high order systems (8th order). Classical and modern control techniques are designed to follow the optimized parameters of the PID controller. Initially, the classical PID controller is designed for the linear system. Owing to the presence of nonlinearity, the GA is used for tuning the PID gains on line for the nonlinear model[12]. In general, the synthesis of PID controller can be depicted by Fig.4, where e is the error, R the reference value, and Y the process output. PID can be described by

$$u=K_{\mathrm{p}}e+K_{\mathrm{r}}\int e\mathrm{d}t+K_{\mathrm{d}}\frac{\mathrm{d}e}{\mathrm{d}t}$$

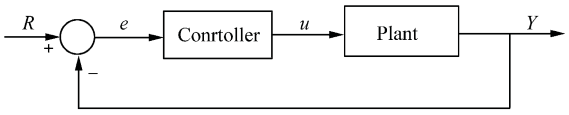

Fig.4 Block diagram of a unity feed back system.

6.2 Characteristics of PID controllers

A proportional controller (K_{p}) has the ability to reduce the rise time but can not eliminate the steady-state error. An integral control (K_{i}) has the capability of removing the steady-state error, but may worsen the transient response. A derivative control (K_{d}) has the power to increase the stability of the system, reduce the overshoots and improve the transient responses. Fig.5 shows step responses for the high order system (8th order) of the EHSAS in a closed loop with unit feed back.

Stable notwithstanding, the system is characterized by very slow responses, so we need to improve it with a classical controller. By using the

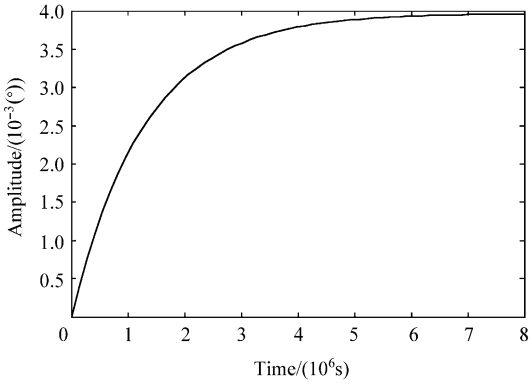

Fig.5 Step responses of EHSAS (closed loop).

SIMULINK program, we simulate the linear model of the EHSAS, design the PID controller and tune it with trail-and-error method to determine the gain parameters K_p, K_i, and K_d. After many trials, the best gain values we found are $K_p = 100$, $K_i = 5$, and $K_d = 0.1$. Fig.9 illustrates the simulation results of the system, from which we find that the steady state error is about 0.025. We accept the PID controller, but it is still required to obviate the steady state error and improve the transient responses by the way of tuning the PID parameters with GA.

7 PID Tuning with GA

Over the past a few years, many different techniques have been developed to acquire the optimum proportional, integral, and derivative control parameters for PID controllers. This article describes the application of GA to optimally tune the three terms of the classical PID controllers to regulate nonlinear processes. Fig.6 shows GA process, which is used in an attempt to overcome the weakness of other conventional approaches in nonlinear cases[13]. Fig.7 shows the block diagram for adjusting the PID parameters via GA on line with the SIMULINK model.

To begin with, the GA should be provided with a population of PID sets. The initial population for choosing PID values ranges from approximately +100% to –100% of the PID values derived from the above-cited trial-and-error method. The size of the initial populations for each of the proportional, integral and derivative parameters is set to be 30,

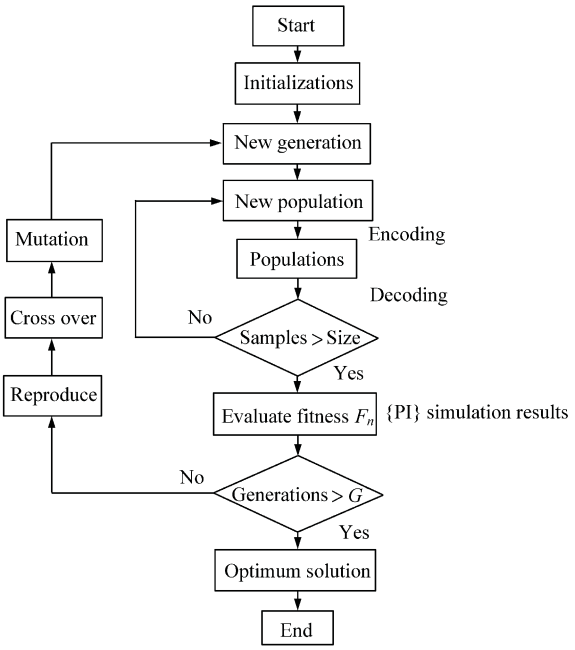

Fig.6 Flow chart of GA functions and process.

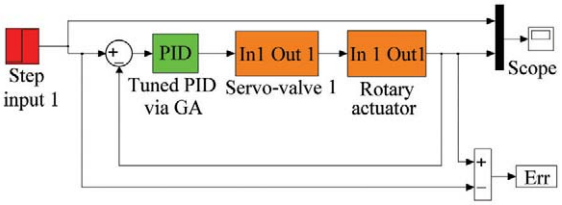

Fig.7 Block diagram of EHSAS to adjust PID parameters via GA on line.

crossover probability $P_c = 0.80$, mutation probability $P_m = 0.10$, and generation $G = 50$.

A fitness evaluation function is needed to calculate the overall responses for each of the sets of PID values and from the responses generates a fitness value for each set of individuals expressed by

$$F(f) = \text{sum}(\text{abs}(R - Y))$$

This fitness evaluation function calculates the sum of errors between the reference and the output of EHSAS for each set of PID values using the SIMULINK program. This program records the system outputs at various sample points. This is done by calculating the integral of the time multiplied by the absolute error value during the time [0, t].

Here the goal is to find a set of PID parameters that will give a minimum fitness value over the period [0, t]. Each set of PID parameters are passed to the fitness evaluation function. The fitness function

obtains the initial responses for each set of solutions. From the responses, it then calculates the fitness value of the above fitness function. The purpose of the GA is to minimize the fitness value. The fitness value for each set of PID parameters will then be returned along with the set of PID values to enable the computation process to continue. Once the PID individuals have been returned, the selection process begins based on the fitness levels of each PID set. This is followed by mutation process and then the crossover process. When this cycle is completed, are produced new sets of PID values which ideally will be at the fitness level higher than the initial population of PID values. These new fitter sets of PID values are then passed to the fitness evaluation function again where the above-mentioned process is repeated. This way the process is cycled unceasingly until the best fitness is achieved (see Fig.8). The off line results of the optimized PID parameters at the assumed population of 30 are: K_p = 493.376 7, K_i = 19.705 9 and K_d = 0.397 3.

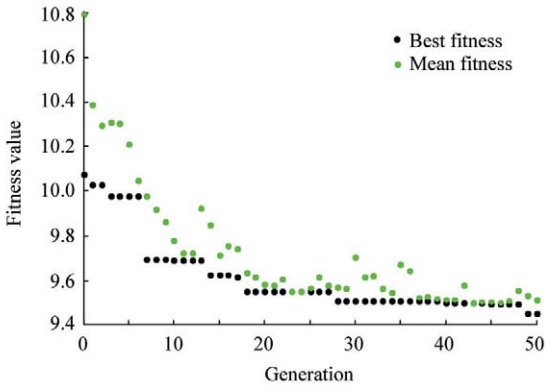

Fig.8 Results of running the GA program with SIMULINK on line to adjust PID parameters.

8 Simulation of the System with PID Controller and Step Inputs

The simulation is carried out on three different controller via GA: compensator controller[14], classical PID controller, and optimized PID controller. Fig.9 shows the step responses of the rotary actuator with the three controller in the simulation and Table 1 lists their comparison.

The classical PID controller and the compensator controller are applied on the linear model while the PID adapted via GA on both models: the linear and the nonlinear. Fig.10 shows the results. The settling time for the nonlinear model (70 ms) is higher than that for the linear one.

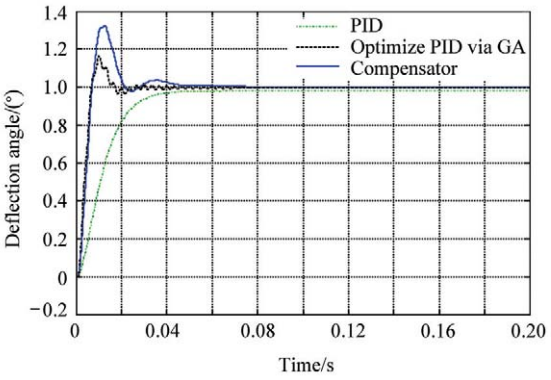

Fig.9 Step responses for three controllers on EHSAS.

Table 1 Comparison of the step responses of three controllers on EHSAS

	T_r/ms	T_s/ms	T_p/ms	E_{ss}/%	P/%
Compensator	4.5	41.5	12.7	0.002	32
Classical PID	22	60	0	0.020	0
Optimize PID	4.15	26	10.1	0.004	16.3

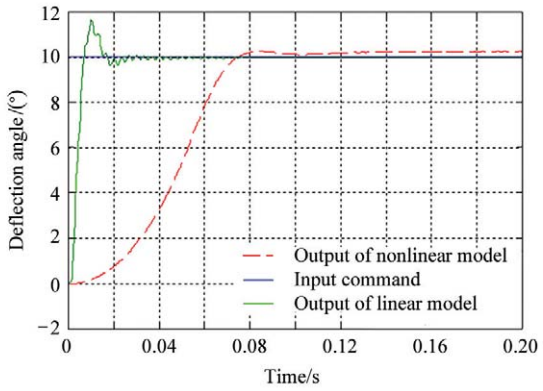

Fig.10 Comparison between the performances of the optimized PID on linear and nonlinear models.

9 Experimental

The experiments are performed on the test rig shown in Fig.11. The experimental parameters are: supplied pressure—190 bars (19 MPa), max deflection angle—10° for each side from zero position, and the max hang moment—10 N·m. The parameters are the same as used in simulation except for the applied load which is 60 N·m in simulation. The result is shown in Fig.12. The experimental results

are higher over shoot than the simulation owing to small applied load and the settling time is 55 ms.

Fig.11 Rig for testing.

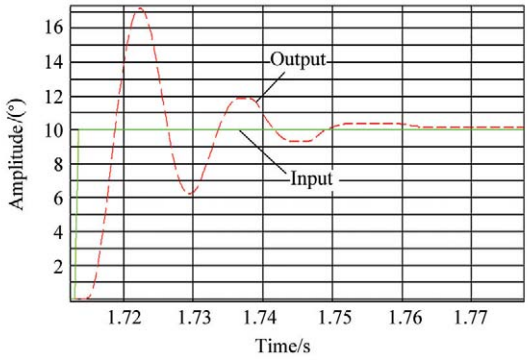

Fig.12 Experimental results.

10 Conclusions

The PID controller design is discussed. The search technique is applied to iteratively modify the parameters of an initial PID controller by using the GA in off line simulation and the gain parameters K_p, K_i, and K_d are optimized. From the simulation, it is understood that, compared with the compensator and classical PID controllers, the optimized PID improve the performances of the hydraulic servo actuator system. The experiment results demonstrate that the outputs of the system with the controller accord well with those with the mathematical model used in the controller design.

References

[1] Bodenhofer U. Genetic algorithms: theory and applications. 2nd Edition. Linz, Austria: Johannes Kepler Universit, 2001.

[2] Rabie M G. Aircraft hydraulic and pneumatic systems. Egypt: Department of Aircraft, Military Technical College, 1995.

[3] Merritt H E. Hydraulic control systems. New York: John Wiley and Sons, 1967.

[4] Liao Y H, Sun C T. An educational genetic algorithms learning tool. IEEE Transaction on Education 2001; 44(2): 1-20.

[5] Ogata K. Modern control engineering. 4th ed. New Jersey: Prentice Hall Publication, 2001.

[6] Chan C W, Hui K. A general actuator saturation compensator in the continuous-time domain. Proceedings of the IEEE International Conference on Industrial Technology. 1994; 206-210.

[7] Zhang P, Yuan M Z, Wang H. Self-tuning PID based on adaptive genetic algorithms with the application of activated sludge aeration process. Proceedings of the 6th World Congress on Intelligent Control and Automation. 2006; Vol.2:9327-9330.

[8] Moradi M H. New techniques for PID controller design. Proceedings of 2003 IEEE Conference on Control Applications. 2003; Vol.2: 903-908.

[9] Yu G R, Hwang R C. Optimal PID speed control of brushless DC motors using LQR approach. IEEE International Conference on Systems, Man and Cybernetics. 2004.

[10] Zou J, Fu X , Yang H Y, et al. A particle swarm optimization approach for PID parameters in hydraulic servo control system. Proceedings of the 6th World Congress on Intelligent Control and Automation. 2006; 369-380.

[11] Mookherjee A. Design and sensitivity analysis of a single stage electro-hydraulic servovalve. Proc of 1st FPNI-PhD Symp. 2000; 71-88.

[12] Elbayomy K M, Jiao Z X. Study of details state space model for a special rotary actuator controlled by two-stage servo valve. Proceedings of 5th International Symposium on Fluid Power Transmission and Control. 2007.

[13] Dinger R H. Engineering design optimization with genetic algorithms. IEEE Northcon/98 Conference Proceedings. 1998; 114-119.

[14] Elbayomy K M, Jiao Z X. Angular position controller and its design model verification for the EHSCS. CADDM 2007; 17: 60-65.

Biography:

Karam M. Elbayomy Born in 1958, he received B.S. and M.S. from Military Technical College, Egypt in 1981 and 2000, respectively. Now he is a Ph.D. candidate in Beijing University of Aeronautics and Astronautics. His main research interest is hydraulic servo actuator system.

E-mail: karam_moh1@yahoo.com